

# GroundedSurg: A Multi-Procedure Benchmark for Language-Conditioned Surgical Tool Segmentation

Tajamul Ashraf<sup>1†</sup>, Abrar Ul Riyaz<sup>\*4</sup>, Wasif Tak<sup>\*2‡</sup>, Tavaheed Tariq<sup>\*4</sup>, Sonia Yadav<sup>4</sup>, Moloud Abdar<sup>3</sup>, and Janibul Bashir<sup>4</sup>

<sup>1</sup> King Abdullah University of Science and Technology (KAUST), Saudi Arabia

<sup>2</sup> Thapar Institute of Engineering and Technology, India

<sup>3</sup> The University of Queensland, Australia

<sup>4</sup> Gaash Research Lab, National Institute of Technology Srinagar, India

**Abstract.** Clinically reliable perception of surgical scenes is essential for advancing intelligent, context-aware intraoperative assistance such as instrument handoff guidance, collision avoidance, and workflow-aware robotic support. Existing surgical tool benchmarks primarily evaluate category-level segmentation, requiring models to detect all instances of predefined instrument classes. However, real-world clinical decisions often requires resolving references to a specific instrument instance based on its functional role, spatial relation, or anatomical interaction capabilities not captured by current evaluation paradigms. We introduce **GroundedSurg**, the first language conditioned, instance-level surgical grounding benchmark. Each instance pairs a surgical image with a natural-language description targeting a single instrument, accompanied by structured spatial grounding annotations including bounding boxes and point-level anchors. The dataset spans ophthalmic, laparoscopic, robotic, and open procedures, encompassing diverse instrument types, imaging conditions, and operative complexities. By jointly evaluating linguistic reference resolution and pixel-level localization, GroundedSurg enables a systematic and realistic evaluation of vision–language models in clinically realistic multi-instrument scenes. Extensive experiments demonstrate substantial performance gaps across modern segmentation and VLMs, highlighting the urgent need for clinically grounded vision–language reasoning in surgical AI systems. Code and data is publically available at <https://github.com/gaash-lab/GroundedSurg>

**Keywords:** Surgical Tool Segmentation · Vision-Language Grounding · Surgical Scene Understanding · Medical Image Benchmark

---

<sup>†</sup> Corresponding author: [tajamul.ashraf@kaust.edu.sa](mailto:tajamul.ashraf@kaust.edu.sa)

<sup>\*</sup> Equal Contribution

<sup>‡</sup> Work done while an intern at Gaash Lab, NIT Srinagar

Table 1: Comparison of surgical tool datasets with respect to grounding capabilities. Our benchmark supports multi-procedure, language conditioning, explicit spatial grounding, instance-level disambiguation, and prompt-based evaluation.

Dataset	Domain	Multi-Proc.	Language	Spatial	Disambig.	Prompt
CaDIS [8]	Cataract	✗	✗	✗	✗	✗
AutoLaparo [30]	Laparoscopic	✗	✗	✗	✗	✗
SISVE [32]	Gastrectomy	✗	✗	✓	✓	✗
EndoVis [26]	Robotic	✗	✗	✗	✗	✗
CholecSeg8k [10]	Cholecystectomy	✗	✗	✗	✗	✗
CholecInstanceSeg [1]	Cholecystectomy	✗	✗	✗	✓	✗
Robust-MIS [22]	MIS	✗	✗	✗	✗	✗
InSeg1 [6]	Ophthalmic	✗	✗	✓	✓	✗
InSeg2 [6]	Ophthalmic	✗	✗	✓	✓	✗
<b>GroundedSurg (Ours)</b>	<b>Multi-procedure</b>	✓	✓	✓	✓	✓

## 1 Introduction

Accurate interpretation of surgical scenes has traditionally been framed as the segmentation and recognition of predefined instrument categories [1, 2, 15]. These category-level formulations have enabled important downstream applications, including workflow analysis, skill assessment, and context-aware assistance systems [23, 28, 29]. However, surgical scene understanding extends beyond class identification. In real operative environments, multiple visually similar instruments often coexist within the same field of view. Their clinical relevance depends not only on category, but also on functional role, spatial configuration, and interaction with surrounding anatomy [6, 26]. Distinguishing the instrument actively dissecting tissue from another instrument of the same type that is idle or retracting therefore requires resolving a context-dependent reference to a specific instance.

Current evaluation paradigms do not assess this capability [6, 8, 23]. Category-level tool segmentation benchmarks measure recognition performance but do not require resolving which specific instance satisfies a procedural description when multiple candidates coexist. As summarized in Table 1, existing surgical tool datasets primarily focus on class-level segmentation and lack integrated support for language conditioning, structured spatial grounding, and instance-level disambiguation across diverse procedures. Conversely, general vision-language grounding benchmarks (e.g., RefCOCO) [17, 18, 33] do not reflect the visual complexity, occlusions, fine-grained instrument morphology, and domain-specific constraints inherent to surgical environments. As a result, grounded, instance-level reasoning in operative scenes remains largely untested. Bridging this gap requires a benchmark that explicitly couples natural-language reference resolution with precise pixel-level instrument localization. Such evaluation must occur under realistic intraoperative conditions, as illustrated in Fig. 1. Such a formulation must support multi-instrument scenes with ambiguity, structured spatial grounding annotations to enforce localization consistency, and evaluation protocols that quantify both grounding accuracy and segmentation precision.

To address this need, we introduce **GroundedSurg**, a grounding-based surgical tool segmentation benchmark consisting of 612 surgical images and 1,071

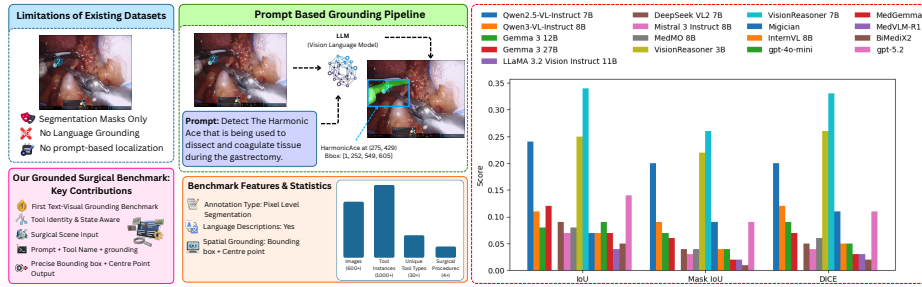


Fig. 1: Overview of **GroundedSurg**. (a) Existing datasets focus on category-level segmentation without language conditioning or instance-level grounding. (b) GroundedSurg introduces natural-language queries with structured spatial annotations for query-conditioned instrument localization. (c) Baseline results reveal substantial performance gaps, highlighting the challenges of grounded surgical perception.

tool-level annotations, that reformulates surgical tool perception as a language-conditioned, instance-level segmentation task. Given a surgical image and a natural-language query describing a specific instrument through its functional role, spatial relation, or anatomical interaction, the objective is to localize and segment the instrument instance satisfying the description. This formulation departs from conventional category-level segmentation by requiring explicit disambiguation among visually similar instruments and grounding of contextual references to a single spatially localized instance. GroundedSurg incorporates structured spatial annotations, including bounding boxes and center points, to quantify localization accuracy at multiple levels of granularity. Bounding boxes enable coarse instance verification, while pixel-level masks assess fine-grained delineation under realistic surgical challenges such as occlusion, specular reflections, motion blur, and instrument overlap. Each image–query pair is treated as an independent evaluation unit, enabling controlled instance-level metric computation in multi-instrument scenes. By unifying natural-language reference, structured spatial grounding, and multi-procedure diversity within a standardized evaluation framework, GroundedSurg establishes a principled benchmark for grounded surgical perception, thereby enabling the next generation of grounding-aware surgical AI systems.

**Contributions.** (1) We reconceptualize surgical tool perception as a grounded vision–language task requiring resolution of context-dependent references to specific instrument instances. (2) We introduce GroundedSurg, a surgical benchmark that systematically couples natural-language descriptions with explicit spatial grounding annotations, including bounding boxes, center points, and pixel-level masks to enable rigorous evaluation of language-conditioned, instance-level localization and segmentation. (3) We curate a diverse, multi-procedure dataset spanning heterogeneous surgical domains and imaging conditions, providing a clinically realistic and reproducible testbed for grounding-aware intraoperative vision systems.

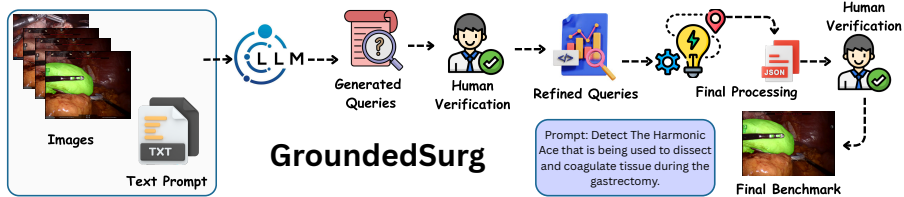


Fig. 2: **GroundedSurg** benchmark pipeline. Surgical images are paired with initial prompts and processed by a vision–language model to generate structured instrument descriptions. All **1071** queries are human and clinician verified for semantic correctness and ambiguity removal. Final annotations are stored in a standardized JSON schema with spatial grounding (bounding box and center point) and segmentation masks.

## 2 GroundedSurg

**Problem Formulation:** GroundedSurg formalizes surgical tool perception as a *language-conditioned, instance-level segmentation* task. Each benchmark instance consists of a surgical image paired with a natural-language description referring to a single target instrument, along with structured spatial grounding annotations and a pixel-level segmentation mask.

Formally, let  $I \in \mathbb{R}^{H \times W \times 3}$  denote a surgical image of height  $H$  and width  $W$ . For each image, a single target instrument instance is defined by: (i) a natural-language query  $T$  describing the instrument through its procedural role, spatial relation, or interaction, (ii) a bounding box  $B = (x_{\min}, y_{\min}, x_{\max}, y_{\max})$ , (iii) a center point  $C = (x_c, y_c)$ , and (iv) a binary segmentation mask  $M \in \{0, 1\}^{H \times W}$ . The objective is to predict a segmentation mask  $\hat{M}$  corresponding to the instrument described by  $T$ , i.e., to learn a mapping  $f(I, T, B, C) \rightarrow \hat{M}$ . Each image–query pair corresponds to exactly one instrument instance. In scenes containing multiple tools, separate instances are constructed for each reference to ensure unambiguous supervision and controlled instance-level evaluation. The spatial annotations  $(B, C)$  act as auxiliary grounding cues to reduce ambiguity and strengthen alignment between linguistic reference and visual localization.

**Benchmark Design:** Unlike conventional category-level segmentation, GroundedSurg requires models to identify and segment a specific instrument instance conditioned on linguistic and spatial cues, enforcing explicit disambiguation when multiple visually similar tools coexist. The bounding box  $B$  provides coarse localization supervision for instance verification, while the center point  $C$  introduces an additional spatial constraint to enhance grounding robustness. Despite these anchors, the primary objective remains precise pixel-level delineation of the referenced instrument, reflecting intraoperative accuracy requirements. Treating each image–query pair as an independent evaluation unit prevents cross-instance interference and enables principled instance-level assessment.

**Dataset Construction:** The dataset aggregates samples from publicly available surgical datasets spanning diverse procedures and imaging conditions, in-

Table 2: Summary statistics of the GroundedSurg dataset.

Statistic	Value
Number of images	~612
Number of annotations	~1,071
Average tools/image	~1.6
Surgical procedures	4
Annotation type	Pixel-level segmentation
Spatial grounding	Box + center point
Language descriptions	Instance-level reference

Table 3: Evaluation metrics used in GroundedSurg.

Metric	Description
<b>Region-Based Metrics</b>	
IoU	$\frac{ M \cap \hat{M} }{ M \cup \hat{M} }$
IoU@0.5/0.9	IoU $\geq 0.5$ / 0.9
mIoU	Mean IoU
Dice	$\frac{2 M \cap \hat{M} }{ M  +  \hat{M} }$
<b>Localization Metrics</b>	
BBBox IoU	Box IoU (pred vs GT)
NDE	Normalized center distance

cluding InSeg1 [6] and InSeg2 [6] (ophthalmic), SISVE [32] (gastrectomy), EndoVis [26] (robotic nephrectomy), and CholecInstanceSeg [1] (laparoscopic cholecystectomy). These sources cover heterogeneous surgical environments, from microsurgical settings with fine instruments to laparoscopic scenes with articulated tools, cluttered backgrounds, and specular reflections. Such diversity introduces realistic challenges including occlusion, instrument overlap, and high visual similarity, enabling evaluation under clinically representative conditions.

**Annotation Protocol:** Each benchmark instance corresponds to a single tool annotation paired with a grounded natural-language prompt and pixel-level segmentation supervision. When multiple tools appear in the same image, each instance is annotated independently. *Instance-Level Supervision.* Each annotation is assigned a unique identifier. The primary supervision signal is a pixel-level mask precisely delineating the visible extent of the target instrument. All masks are aligned to original image resolution and verified for geometric consistency. Auxiliary spatial grounding information, including bounding box and center point annotations, provides structured localization cues. *Language Grounding:* Queries are generated using Qwen-2.5 VL-Instruct [27] conditioned on visual content and spatial annotations. Each annotation includes (i) a textual description of the target instrument, (ii) explicit spatial grounding via bounding box and center point references, and (iii) a reasoning cue specifying the segmentation objective.

**Clinical Validation:** The dataset follows a semi-automated, clinically validated pipeline. Initial queries generated by a vision–language model are reviewed and verified by clinicians to eliminate hallucinations, correct semantic inconsistencies, and ensure alignment with surgical context. Refined queries are standardized and integrated into a unified JSON schema, followed by a second round of human validation to guarantee accurate prompt–mask alignment and spatial consistency.

**Dataset Statistics:** The dataset contains approximately **612 surgical images** and **1,071 tool-level annotations**. Because multiple instruments may appear per image, annotation count exceeds image count. The dataset spans four procedures and diverse imaging conditions. All annotations include pixel-level masks, bounding boxes, center points, and natural-language descriptions, establishing a moderate-scale yet fine-grained benchmark for grounding-based surgical segmentation under realistic clinical variability.

Table 4: Quantitative comparison of vision-language models on GroundedSurg under a unified query-conditioned segmentation protocol. Best results are shown in **bold**, second-best are underlined.

Model	Params	IoU@0.1	IoU@0.3	BBox IoU	mIoU@0.1	mIoU@0.3	Mask IoU	NDE ↓	Dice
<i>Open-Source Models</i>									
Qwen2.5-VL-Instruct [27]	7B	<b>0.52</b>	<b>0.33</b>	<u>0.24</u>	<b>0.26</b>	<b>0.22</b>	<u>0.20</u>	<u>1.45</u>	<u>0.20</u>
Qwen3-VL-Instruct [3]	8B	0.36	0.13	0.11	0.17	0.12	0.09	1.78	0.12
Gemma 3   [7] (12B)	12B	0.28	0.09	0.08	0.13	0.09	0.07	<u>1.45</u>	0.09
Gemma 3 [7] (27B)	27B	<u>0.43</u>	0.11	0.12	0.11	0.07	0.06	1.52	0.07
LLaMA 3.2 Vision [9]	11B	0.02	0.00	0.00	0.01	0.00	0.00	2.90	0.00
DeepSeek VL2 [31]	7B	0.28	0.10	0.09	0.06	0.05	0.04	1.89	0.05
Mistral 3 [13]	8B	0.27	0.06	0.07	0.07	0.04	0.03	1.89	0.04
<i>Reasoning-Oriented Models</i>									
VisionReasoner (3B) [14]	3B	0.20	0.06	0.25	0.23	0.03	0.22	1.39	0.26
VisionReasoner (7B) [14]	7B	0.32	<u>0.20</u>	<b>0.34</b>	<u>0.25</u>	<u>0.12</u>	<b>0.26</b>	<b>1.05</b>	<b>0.33</b>
Migician [12]	7B	0.19	0.08	0.07	0.16	0.12	0.09	1.72	0.11
InternVL [4]	8B	0.29	0.05	0.07	0.08	0.05	0.04	1.69	0.05
<i>Medical-Domain Models</i>									
MedMO [5]	8B	0.33	0.04	0.08	0.08	0.05	0.04	1.50	0.06
MedGemma [24]	4B	0.29	0.04	0.07	0.05	0.03	0.02	1.88	0.03
MedVLM-R1 [20]	2B	0.13	0.01	0.04	0.05	0.03	0.02	2.16	0.03
BiMediX2 [19]	8B	0.23	0.04	0.05	0.07	0.02	0.01	2.11	0.02
<i>Closed-Source Models</i>									
GPT-4o-mini [16]	-	0.35	0.04	0.09	0.08	0.05	0.04	1.63	0.05
GPT-5.2 [25]	-	0.39	<u>0.20</u>	0.14	0.16	0.12	0.09	1.95	0.11

**Evaluation Protocol:** Performance is evaluated at the instance level, treating each image–query pair independently.

*Region-Based Metrics:* Segmentation quality is measured using Intersection over Union (IoU), defined as  $\text{IoU} = \frac{|M \cap M|}{|M \cup M|}$ . We report IoU@0.5, IoU@0.9, mean IoU (mIoU), and Dice coefficient to assess overlap and boundary fidelity.

*Localization Metrics:* Spatial grounding accuracy is evaluated using Bounding Box IoU and Normalized Distance Error (NDE) between predicted and ground-truth center points. All metrics are averaged across instances for systematic comparison of language-conditioned segmentation models in multi-instrument surgical scenes.

### 3 Experiments

**Experimental Setup:** We evaluate GroundedSurg under a unified language-conditioned instance segmentation protocol, where models predict structured localization outputs (bounding box and center point) that are projected onto a frozen SAM-based backend to obtain final masks. All models are evaluated in a zero-shot setting without fine-tuning, and performance is reported at the instance level for each image–query pair.

**Comparison Across Vision–Language Models:** Table 4 presents quantitative comparisons across open-source, reasoning-oriented, medical-domain, and closed-source models under the unified protocol. Across model families, performance remains limited under stricter overlap thresholds. While moderate IoU@0.1 values are observed for certain models, accuracy degrades sharply at

**Table 5.** Comparison of representative models under SAM2 [21] and SAM3 [11] as segmentation models after detections from VLMS. Best results are highlighted in **bold**, second-best are underlined.

Model	SAM2		SAM3	
	Mask IoU	Dice	Mask IoU	Dice
Qwen2.5	<b>0.22</b>	<b>0.26</b>	<u>0.20</u>	0.20
Qwen3	0.12	0.16	0.09	0.12
Gemma 3 27B	0.03	0.04	0.06	0.07
MedMO	0.00	0.01	0.04	0.06
gpt-5.2	0.04	0.06	0.09	0.11
VR-7B	<u>0.17</u>	<u>0.19</u>	<b>0.26</b>	<b>0.33</b>

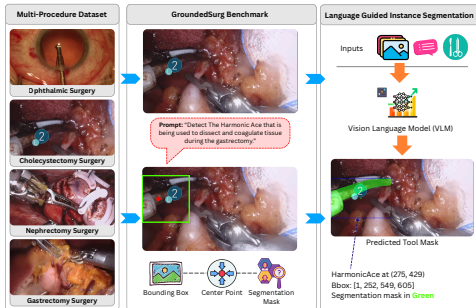


**Fig. 3.** GroundedSurg components.

Table 5: Sensitivity analysis under two prompt formulations. Best results per metric are shown in **bold**, second-best are underlined.

Model	Prompt1					Prompt2				
	IoU@0.1	IoU@0.3	BBox IoU	NDE ↓		IoU@0.1	IoU@0.3	BBox IoU	NDE ↓	
Qwen2.5-VL-7B [27]	<u>0.52</u>	<u>0.33</u>	0.24	1.45		0.38	0.09	0.11	<u>1.43</u>	
Qwen3-VL-8B [3]	0.36	0.13	0.11	1.78		0.11	0.02	0.09	2.94	
Gemma3-27B [7]	0.43	0.11	0.12	1.52		0.42	0.08	0.10	1.51	
InternVL-8B [4]	0.29	0.05	0.07	1.69		0.37	0.09	0.10	1.42	
MedGemma-4B-it [24]	0.29	0.04	0.07	1.88		0.21	0.06	0.07	1.91	
VisionReasoner-7B [14]	0.32	0.08	<b>0.34</b>	<b>1.05</b>		<b>0.58</b>	<b>0.39</b>	<u>0.31</u>	1.14	

higher thresholds (IoU@0.3 and beyond), indicating that coarse localization is occasionally achievable but precise boundary alignment remains challenging.

Among open-source models, Qwen2.5-VL [27] achieves relatively strong coarse grounding performance but exhibits reduced accuracy under stricter overlap criteria, suggesting limited fine-grained spatial precision. In contrast, reasoning-oriented models demonstrate improved localization consistency. VisionReasoner-7B [14] achieves the highest BBox IoU and Dice scores, indicating stronger spatial grounding and mask fidelity, suggesting that structured reasoning enhances robustness under surgical ambiguity. Medical-domain models do not consistently outperform general-purpose models, indicating that domain pretraining alone does not guarantee improved instance-level grounding. Closed-source systems achieve competitive but not dominant performance, reinforcing the overall difficulty of the benchmark.

**Segmentation Backend Analysis.** To assess the impact of the promptable segmentation backend, we compare representative models under different frozen segmentation models. Table 4 shows that segmentation quality varies substantially between SAM2 [21] and SAM3 [11]. While some models benefit from improved mask projection under SAM3, others show marginal gains. Notably, VisionReasoner exhibits a pronounced improvement under SAM3, suggesting stronger compatibility between accurate localization outputs and advanced mask decoding. These results highlight the tight coupling between grounding accuracy and segmentation projection in the overall pipeline.

As shown in Table 5, general-purpose vision-language models exhibit significant performance variation across prompt styles. For example, Qwen3-VL [3] and several other models experience notable drops in IoU and BBox IoU under the

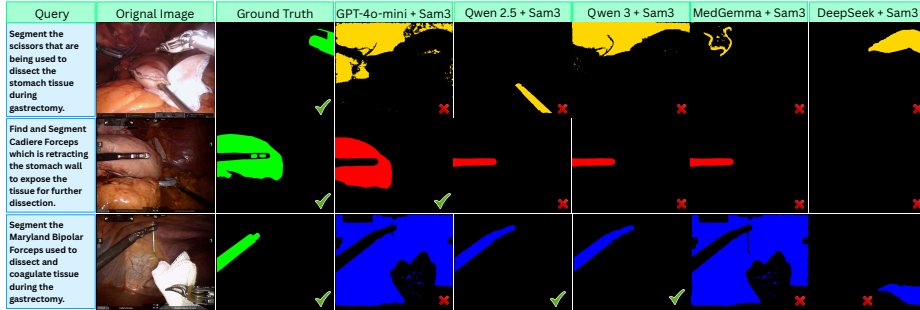


Fig. 3: Qualitative comparison on GroundedSurg showing that reasoning-oriented models produce more spatially precise masks than general-purpose models when projecting structured localization outputs onto a frozen segmentation backend, particularly in multi-instrument and visually cluttered scenes.

alternate prompt. In contrast, reasoning-oriented models demonstrate greater robustness; VisionReasoner-7B maintains and even improves performance under Prompt2, indicating stronger semantic grounding and reduced reliance on rigid prompt structure. These findings suggest that prompt engineering remains critical for general-purpose multimodal models, whereas reasoning-focused architectures exhibit improved invariance to linguistic rephrasing.

**Qualitative Analysis.** Figure 3 presents qualitative comparisons across representative models. General-purpose vision–language models, which do not directly perform segmentation, often generate coarse or inaccurate spatial localizations in cluttered surgical scenes. When these predicted regions are subsequently provided to SAM3 for mask generation, the resulting segmentations remain imprecise, with inaccurate boundaries and contextual leakage—particularly in multi-instrument settings. These qualitative observations are consistent with the quantitative trends reported in Table 4.

**Effect of Prompt Tuning.** The prompt sensitivity results (Table 5) confirm that segmentation performance is strongly influenced by instruction structure. While many models show instability under minor rephrasing, reasoning-oriented models maintain consistent grounding behavior, indicating that explicit spatial reasoning improves robustness to linguistic variability.

**Segmentation Projection Effects.** The comparison between SAM2 and SAM3 (Table 4) further shows that mask quality depends not only on localization accuracy but also on backend projection characteristics. Improvements in mask decoding disproportionately benefit models with stronger localization, emphasizing the importance of evaluating grounding and segmentation components.

## 4 Conclusion

We introduced GroundedSurg, a grounding-based benchmark that reformulates surgical instrument perception as a language-conditioned, instance-level segmentation task. By integrating natural-language references with structured spatial

grounding and pixel-level masks, we advance beyond category-level recognition toward context-dependent, clinically meaningful localization across diverse procedures. Experiments show that current multimodal models struggle with reliable instance-level grounding in complex surgical scenes. While coarse localization is occasionally achievable, precise boundary delineation and robustness to prompt variation remain limited. GroundedSurg provides a standardized and clinically relevant testbed for advancing grounding-aware intraoperative vision and highlights the need for models that better integrate linguistic reasoning with fine-grained spatial perception.

## References

1. Alabi, O., Toe, K.K.Z., Zhou, Z., et al.: Cholecinstanceseg: A tool instance segmentation dataset for laparoscopic surgery. *Scientific Data* **12**, 825 (2025). <https://doi.org/10.1038/s41597-025-05163-w>
2. Allan, M., et al.: 2017 robotic instrument segmentation challenge (2019), <https://arxiv.org/abs/1902.06426>
3. Bai, S., Cai, Y., Chen, R., Chen, K., Chen, X., Cheng, Z., Deng, L., Ding, W., Gao, C., Ge, C., et al.: Qwen3-vl technical report. arXiv preprint arXiv:2511.21631 (2025)
4. Chen, Z., Wu, J., Wang, W., Su, W., Chen, G., Xing, S., Zhong, M., Zhang, Q., Zhu, X., Lu, L., et al.: Internvl: Scaling up vision foundation models and aligning for generic visual-linguistic tasks. In: *Proceedings of the IEEE/CVF conference on computer vision and pattern recognition*. pp. 24185–24198 (2024)
5. Deria, A., et al.: Medmo: Grounding and understanding multimodal large language model for medical images. arXiv preprint arXiv:2602.06965 (2026)
6. Fox, M., Taschwer, M., Schoeffmann, K.: Pixel-based tool segmentation in cataract surgery videos with mask R-CNN. In: *33rd IEEE International Symposium on Computer-Based Medical Systems, CBMS 2020, Rochester, MN, USA, July 28-30, 2020*. pp. 565–568. IEEE (2020). <https://doi.org/10.1109/CBMS49503.2020.00112>
7. Gemma Team: Gemma 3 technical report (2025), <https://arxiv.org/abs/2503.19786>
8. Grammatikopoulou, M., Flouty, E., Kadkhodamohammadi, A., et al.: Cadis: Cataract dataset for image segmentation. arXiv preprint arXiv:1906.11586 (2019), <https://arxiv.org/abs/1906.11586>
9. Grattafiori, A., Dubey, A., Jauhri, A., Pandey, A., Kadian, A., Al-Dahle, A., Letman, A., Mathur, A., Schelten, A., Vaughan, A., et al.: The llama 3 herd of models. arXiv preprint arXiv:2407.21783 (2024)
10. Hong, W.Y., Kao, C.L., Kuo, Y.H., Wang, J.R., Chang, W.L., Shih, C.S.: Cholecseg8k: A semantic segmentation dataset for laparoscopic cholecystectomy based on cholec80 (2020), <https://arxiv.org/abs/2012.12453>
11. Jiang, C., et al.: Medical sam3: A foundation model for universal prompt-driven medical image segmentation. arXiv preprint arXiv:2601.10880 (2026), <https://arxiv.org/abs/2601.10880>
12. Li, Y., Huang, H., Chen, C., Huang, K., Huang, C., Guo, et al.: Migician: Revealing the magic of free-form multi-image grounding in multimodal large language models. In: *Findings of the Association for Computational Linguistics (ACL 2025)*. pp. 9845–9867 (2025)

13. Liu, A.H., Khandelwal, K., Subramanian, S., Jouault, V., Rastogi, A., Sadé, A., Jeffares, A., Jiang, A., Cahill, A., Gavaudan, A., et al.: Ministral 3 (2026)
14. Liu, Y., Qu, T., et al.: Visionreasoner: Unified reasoning-integrated visual perception via reinforcement learning. arXiv preprint arXiv:2505.12081 (2025)
15. Maier-Hein, L., et al.: Surgical data science for next-generation interventions. *Nature Biomedical Engineering* **1**, 691–696 (2017). <https://doi.org/10.1038/s41551-017-0132-7>
16. Mao, J., Huang, J., Toshev, A., Camburu, O., Yuille, A.L., Murphy, K.: Generation and comprehension of unambiguous object descriptions. In: Proceedings of the IEEE conference on computer vision and pattern recognition. pp. 11–20 (2016)
17. Mao, J., et al.: Generation and comprehension of unambiguous object descriptions pp. 11–20 (2016)
18. Mao, J., et al.: Generation and comprehension of unambiguous object descriptions. In: Proceedings of the IEEE conference on computer vision and pattern recognition. pp. 11–20 (2016)
19. Mullappilly, S.S., et al.: Bimedix2: Bio-medical expert lmm for diverse medical modalities (2024), <https://arxiv.org/abs/2412.07769>
20. Pan, J., et al.: Medvlm-r1: Incentivizing medical reasoning capability of vision-language models (vlms) via reinforcement learning. arXiv preprint arXiv:2502.19634 (2025)
21. Ravi, N., et al.: Sam 2: Segment anything in images and videos (2024), <https://arxiv.org/abs/2408.00714>
22. Ross, T., Reinke, A., Full, P.M., Wagner, M., Kenngott, H., Apitz, M., Hempe, H., et al.: Robust medical instrument segmentation challenge 2019 (2020), <https://arxiv.org/abs/2003.10299>
23. Sachdeva, B., Akash, N., Ashraf, T., Mueller, S., Schultz, T., Wintergerst, M.W.M., Prasad, N.S., Murali, K., Jain, M.: Phase-informed tool segmentation for manual small-incision cataract surgery (2024), <https://arxiv.org/abs/2411.16794>
24. Sellergren, A., et al.: Medgemma technical report. arXiv preprint arXiv:2507.05201 (2025)
25. Singh, A., Fry, A., Perelman, A., Tart, A., Ganesh, A., El-Kishky, A., McLaughlin, A., Low, A., Ostrow, A., Ananthram, A., et al.: Openai gpt-5 system card. arXiv preprint arXiv:2601.03267 (2025)
26. Sun, L., Chen, X.: Pixel-wise contrastive learning for multi-class instrument segmentation in endoscopic robotic surgery videos using dataset-wide sample queues. *IEEE Access* **12**, 156867–156877 (2024)
27. Team, Q.: Qwen2.5: A party of foundation models (September 2024), <https://qwenlm.github.io/blog/qwen2.5/>
28. Twinanda, A.P., Shehata, S., Mutter, D., Marescaux, J., de Mathelin, M., Padoy, N.: Endonet: A deep architecture for recognition tasks on laparoscopic videos (2016), <https://arxiv.org/abs/1602.03012>
29. Wang, Q., Zhao, S., Xu, Z., Zhou, S.K.: Lacoste: Exploiting stereo and temporal contexts for surgical instrument segmentation. *Medical Image Analysis* **99**, 103387 (11 2024). <https://doi.org/10.1016/j.media.2024.103387>
30. Wang, Z., et al.: Autolaparo: A new dataset of integrated multi-tasks for image-guided surgical automation in laparoscopic hysterectomy (2022), <https://arxiv.org/abs/2208.02049>
31. Wu, Z., et al.: Deepseek-vl2: Mixture-of-experts vision-language models for advanced multimodal understanding (2024), <https://arxiv.org/abs/2412.10302>

32. Yoon, J., et al.: Surgical scene segmentation using semantic image synthesis with a virtual surgery environment: Enhanced with object size-aware random crop and background label enhancement for photo-realistic synthesis (March 2024), <https://sisvse.github.io/>
33. Yu, L., Poirson, P., Yang, S., Berg, A.C., Berg, T.L.: Modeling context in referring expressions. CoRR **abs/1608.00272** (2016), <http://arxiv.org/abs/1608.00272>